ZANCO Journal of Pure and Applied Sciences
The official scientific journal of Salahaddin University-Erbil
https://zancojournals.su.edu.krd/index.php/JPAS

ISSN (print):2218-0230**, ISSN (online):** 2412-3986**, DOI: http://dx.doi.org/10.21271/zjpas**

RESEARCH PAPER

Comparative Investigation of the Spherical Acoustic Microbubble Models in an Unbounded Liquid.

Narmeen N. Nadir[1], Kawa M.A. MANMI[2]

[1]Department of Petroleum Equipment, Erbil Technology Institute, Erbil Polytechnic University
[2] Department of Mathematics, College of Science, Salahaddin University-Erbil, Kurdistan Region, Iraq

A B S T R A C T:
Microbubble oscillating associated with many applications in biomedical and engineering sectors. The spherical oscillations of a single microbubble submerged in a quiescent liquid exerted by an acoustic force can be governed either by the Rayleigh-Plesset (RP) equation or by the Keller-Miksis (KM) equation under different physical assumptions. In this paper, both models were numerically and analytically analyzed, and the systematic parametric study was performed. The viscosity and compressibility effects and linearization in both models were investigated with the aids of MATLAB and Maple tools. In KM, the effects of the linear and nonlinear equations of states (EOS) compared for updating density with time. At the minimum bubble radius, the liquid viscosity surrounding bubble surface expected to be decreased due to rising in temperature. This leads to effects the maximum bubble radius for upcoming cycles.

KEY WORDS: Cavitation, Bubble Oscillation, Rayleigh-Plesset equation, Keller-Miksis, numerical methods for ODEs.
DOI: http://dx.doi.org/10.21271/ZJPAS.32.4.10
ZJPAS (2020) , 32(4);82-88 .

1. INTRODUCTION

Cavitation phenomena can be defined as the formation, rapid expansion and shrink of gas or vapor bubbles in a liquid due to reduction in liquid pressure locally to below the statured vapor pressure (Franc and Michel, 2006). This often occurs in many engineering processes induced by rapid changes in liquid situations. For instance, when a liquid moves in a pipe with sudden decrease in the pipe's cross-section. Classically, cavitation is undesirable as it leads to surface erosion, increase noise, reduction of efficiency and damage in mechanical engines.

* **Corresponding Author:**
Kawa M. A. MANMI
E-mail: kawa.aziz@su.edu.krd
Article History:
Received: 19/03/2020
Accepted: 10/05/2020
Published: 08/09 /2020

industry, semiconductor cleaning, targeted drug delivery, biomedical treatments like kidney stones (Kerabchi et al., 2018) disintegration, promoting chemical processes and the removal of bacterial biofilm in medical and dental applications (Vyas et al., 2019, Manmi et al., 2020). Acoustic waves might be used in majority of these applications, to generate and enhance the cavitation in the fluid, hence this kind of cavitation is called acoustic cavitation.

The bubble and droplet usually take a spherical shape due to surface tension force without interaction with any neighbouring particles or structures. Therefore, understanding spherical bubble oscillation is crucial, as in many situations the bubble's shape during oscillation, can be approximated as spherical. On the other hand, the microbubble surface is stabilized in biomedical applications, to remain spherical and

prevent dissolution. This can usually be done by coating the bubble's surface with a shell typically made from lipid, protein, or polymer, commonly known as ultrasound contrast agent (Wang et al., 2015).

The oscillations of a single bubble have been widely studied theoretically, experimentally, and numerically for about one century. The first formal attempt in 1917 was done by Rayleigh who described the growth and contraction of a spherical or approximately spherical bubble in an incompressible and Newtonian liquid without considering the surface tension force and liquid viscosity effects at infinite container. The pressure difference between pressure inside the bubble and the external atmospheric pressure of the surrounding liquid is driving the bubble motion. His works was motivated to investigate cavitation damage and erosion on a ship propeller (Plesset and Prosperetti, 1977).

In 1949, Plesset (Plesset and Prosperetti, 1977) modified his equation to include surface tension and viscous effects under the same assumptions. This leads to introduce the famous and basic Rayleigh-Plesset equation for radial bubble motion. The main weakness of the RPE, is the lack of consideration for the compressibility effects for the surrounding liquid, which means lack of ability to consider damping amplitude of oscillation from acoustic radiation. The shockwaves might be formed due to this acoustic radiation particularly when the bubble is under violent oscillation. Eventually, it might have a large impact on the bubble dynamics.

In 1956, Keller and Kolodner (Keller and Kolodner, 1956) rederived the equation to consider the compressibility (small density variation). In 1980 their equation was developed by Keller and Miksis (Keller and Miksis, 1980) to include the standing acoustic wave. This essential equation for spherical bubble oscillations in a compressible fluid with or without an external acoustic force, is called the Keller-Miksis equation (Keller and Miksis, 1980).

In this study, viscosity and compressibility effects have been investigated in the RP and KM equations. The initial viscosity is increased from μ=0.001 to 0.004 and 0.008 kg (m s)-1. Also, at the end of the first cycle of oscillation the viscosity is increased from μ=0.001 to 0.004 and 0.008 kg (m s)-1 because during bubble collapse, the inertia of the surrounding water causes high pressure and high temperature, reaching around 10,000 kelvins in and surrounding the bubble's surface. Hence, we investigated this viscous change and compared it with constant viscosity during the whole simulation. In the KM model the density is not constant, as it is based on the weakly compressible theory. Therefore, linear and nonlinear equations of state have been used to update the density at each time step and compare the results. Furthermore, for a small amplitude of bubble oscillations the RP and KM are approximated to the linear second order differential equation so we're able to find the analytical solution and compare them with each other.

2. MATHEMATICAL MODELLING

Here we introduce the governing equation of spherical bubble dynamics in an incompressible fluid. For a Newtonian fluid, the governing equation reduces to the Rayleigh–Plesset equation (RPE) (Plesset and Prosperetti, 1977), which represents a second order non-linear ordinary differential equation with dependent variable R (bubble radius) and independent variable t (time).

$$\ddot{R}R + \frac{3}{2}\dot{R}^2 = \frac{1}{\rho}\left(p_b(t) + p_v - p_\infty(t) - \frac{4\mu}{R}\dot{R} - \frac{2\sigma}{R}\right), \quad (1)$$

where $\dot{R}$ and $\ddot{R}$ are velocity and acceleration of the bubble which are function of time (t), ρ and μ are the density and viscosity of the liquid, σ is surface tension coefficient and p_v is vapour pressure. All parameters were considered as constant throughout this paper, unless otherwise stated. For oscillating bubble without acoustic field, $p_\infty(t)$ is basically a constant p_∞ and is usually considered as ambient pressure. In this paper, we investigate the more interesting case and includes the effects of the pressure $P(t)$ of a planar acoustic standing wave. Thus, the far-field pressure is,

$$p_\infty(t) = p_\infty + P(t) = p_\infty(1 + a\cos(\omega t + \phi)), \quad (2)$$

where ω is the angular frequency of the acoustic wave, and $a << 1$ is the pressure perturbation

amplitude and ϕ is the wave phase. It can be assuming that the pressure inside bubble p_b follows Dalton's law consist in two parts which are vapour pressure p_v and partial gas pressure. Furthermore, we assume that there is no heat and mass transfer. Therefore, the bubble pressure can be written as (Brennen, 2014, Grieser *et al.*, 2015),

$$p_b = p_{g0}\left(\frac{R_0}{R}\right)^{3k}, \quad (3)$$

where k is called ratio of specific heat. For adiabatic system, it is real and approximately constant between 1 and 2; and p_{g0} is the gas pressure inside bubble at some bubble size R_0. Using $\Delta p = p_\infty - p_v$ and R_0 to nondimensionalize all variables in Equation (1) (Wang and Manmi, 2014, Wang et al., 2015, Abo *et al.*, 2018) which leads;

$$\ddot{R}_* R_* + \frac{3}{2}\dot{R}_*^2 = \varepsilon R_*^{-3k} + 1 - p_{a*}\cos(\omega_* t_* + \phi) - \frac{4}{Re\, R_*}\dot{R}_* - \frac{2\sigma_*}{R_*}. \quad (4)$$

Keller-Miksis equation (KM) is a second order nonlinear ordinary differential equation with the dependant variable R_* and independent variable time t_* which describes large amplitude oscillations of bubble in a Newtonian liquid and takes liquid compressibility as a first order approximation into account. It is expressed as,

$$\ddot{R}R\left(1-\frac{\dot{R}}{C}\right) + \frac{3}{2}\dot{R}^2\left(1-\frac{\dot{R}}{3C}\right) = \frac{1}{\rho}\left[\left(1-\frac{\dot{R}}{C}\right)P_L + \frac{R}{C}\dot{P}_L\right], \quad (5)$$

where *C* is speed of sound in the liquid and

$$P_L = p_b + p_v - p_\infty(t) - \frac{4\mu}{R}\dot{R} - \frac{2\sigma}{R}. \quad (6)$$

If *C* approaches to ∞ equation (5) reduce to equation (1). In order to consider the compressibility; the density must be varying to transfer the wave energy between particles. Equations of states (EOS) are mathematical relationships between the variables of temperature, pressure, volume and moles of pure substance or a mixture (Smith *et al.*, 2013). There are several EOS to formulate this variation, but in adiabatic system density must be only the function of pressure. It can be simply a linear with pressure for ideal gas or it can be nonlinear. A very accurate equation of state for liquids in bubble dynamics is described by Tait (Brennen, 2014, Gilmore, 1952, Koch *et al.*, 2016), and states:

$$\rho = \rho_0\left(\frac{p_L + B}{p_\infty + B}\right)^{\frac{1}{n_T}}, \quad (7)$$

p_∞ and ρ_∞ are the ambient pressure and the equilibrium density of the liquid respectively, $n_T = 7.15$ and $B = 3046 \times 10^5$ are knows as Tait exponent and Tait pressure respectively.

$$\frac{1}{C^2} = \frac{d\rho}{dp_L} = \frac{\rho_l}{\left(\frac{\rho_l}{\rho_\infty}\right)^{n_T} n_T\,(p_\infty + B)}. \quad (8)$$

Equations (1) and (5) cannot be solved analytically except for very few special cases (Lauterborn and Kurz, 2010). However, accurate and stable approximate solutions can be obtained by using fourth order Runge-Kutta scheme (RK4). We used Matlab function ode45 here with the options of controlling the relative error and maximum time step to achieve stable numerical solution even for a high frequency microbubble oscillation in a short period time.

3. PARAMETRIC INVESTIGATION

3.1. Numerical investigation of RPE

In this section, parametric studies were performed to investigate the effects of viscosity for the first five cycles on the minimum and maximum bubble radius, time period of each cycle. The parameters in this paper are $R_0 = 4.5$ μm, f =26.5 kHz, $p_{a*} = 1.2$ $\sigma = 0.073$ N/m, $\lambda = 1.4$, $\rho =$ 998 kg/m^3, $p_v = 0.023 p_\infty$, $p_\infty = 1.013$MPa and $\varepsilon = 1 + 2\sigma_*$ (Prosperetti and Hao, 1999, Yuan *et al.*, 1998, Wang, 2016) Figure 1 shows the bubble radius history for three different viscosity μ=0.001, 0.004, 0.008 kg (m s)$^{-1}$, but in Figure 1b, initially in all three cases μ=0.001 and at the end of the first cycle it was changed to 0.004, and 0.05 (dashed red and dotted black lines respectively). Many researchers reported that, in the acoustic cavitation sonoluminescence phenomenon occurs which is releasing thermal energy from the bubble collapse as light emission. The temperature exceeds several thousand Kelvins. On the other hand, the viscosity decreases with increasing temperature. Therefore, based on this we reduced the viscosity at the end of the first collapse in Figure 1b. As can be noted in Figure 1a, b; the maximum bubble radius and time period at each cycle decrease with increasing viscosity and in all cases the bubble radius rapidly damping due to viscosity expect the cases μ=0.001 which is gradually damping.

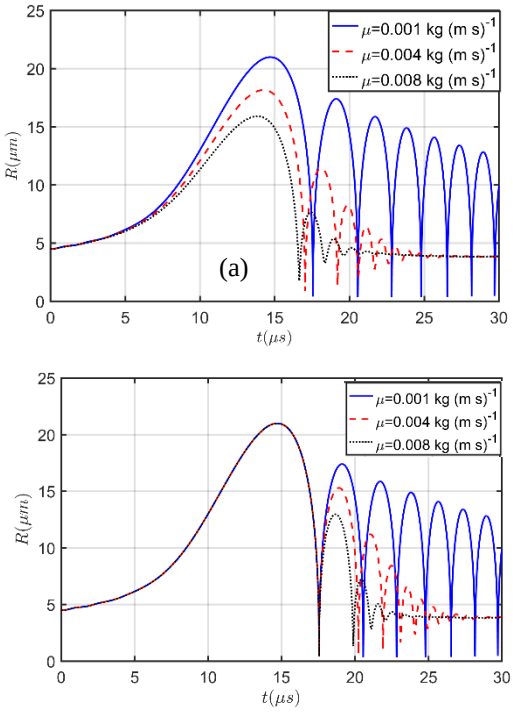

Figure 1: The Bubble radius versus time obtained from numerical solution of RPE with the parameters $R_0 =$ 4.5 μm, f =26.5 kHz, $p_{a*} = 1.2$ $\sigma = 0.073$ N/m, $\lambda = 1.4$, $\rho = 998$ kg/m^3, $p_v = 0.023p_\infty$, $p_\infty = 1.013$ MPa and $\varepsilon = 1 + 2\sigma_*$. (a) Constant viscosity is μ=0.001, 0.004, 0.008 kg (m s)$^{-1}$. (b) Initial viscosity is μ=0.001 kg (m s)$^{-1}$, at the end of first cycle it changed to 0.004 kg (m s)$^{-1}$ (dashed red line) and 0.008 kg (m s)$^{-1}$ (dotted black line).

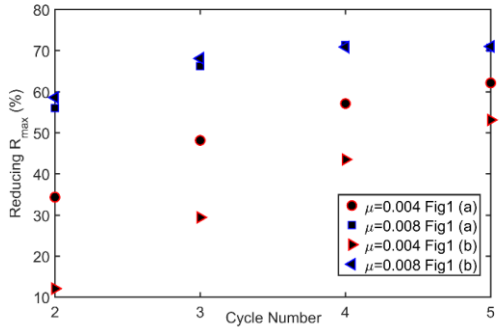

Figure 2: Reducing rate of maximum bubble radius for the cases in Figure 1.

Figure 2 shows that the decreasing rate of maximum bubble radius for the cases μ=0.004 and μ=0.008 to the cases μ=0.001. When the liquid viscosity relatively large as in the case μ=0.008, difference between rate of reductions in the maximum bubble radius is not significant (blue marks) due to dominant the viscose force effects however, in the case μ=0.004 the difference is significant (red marks).

3.2. Numerical investigation of KM

In this section, nonlinear spherical oscillations of microbubble studied for different scenarios. The compressibility of the fluid is usually measured based on Mach number (Ma) which can be expressed by u/C where u is the velocity of the bubble surface in the fluid and C is the speed of sound in that fluid which is about 1465 m/s at 20^o Celsius. We used the same parameters in the case of Figure 1 unless otherwise stated.

Firstly, following other researchers in the Literature, we assume that the Ma is constant throughout the whole simulation. Therefore, $u_{\text{ref}} = \sqrt{\frac{p_\infty - p_v}{\rho}} \approx 10$ is used with three different viscosities μ=0.001, 0.004, and 0.008 kg (m s)$^{-1}$. Figure 3a and 3b show the bubble radius history with viscosity either initially or at the end of the first cycle changed respectively. Clearly, the maximum bubble radius R_{max} rapidly decreasing and minimum bubble radius R_{min} increasing with time due to both viscosity and compressibility effects. In Figure 3a the decreasing rate of R_{max} for μ=0.001 in the 2nd, 3rd, 4th and 5th cycle is about 44 %, 21%, 15% and 11%; for μ=0.004 about 45%, 27%, 20% and 11%; and for μ=0.008 50%, 31%, 18% and 9% respectively. For these data we can conclude that in the 2nd and 3rd cycle decreasing rate of R_{max} increase with μ, but in the 4th and 5th do not follow this trend.

Figure 4 shows the changing rate of R_{max} for the cases shown in the Figure 3 with cycle number. We can only observe some discrepancy at the second cycle between cases in Figure 3a and Figure 3b. Further both cases are approached to each other with the cycles number.

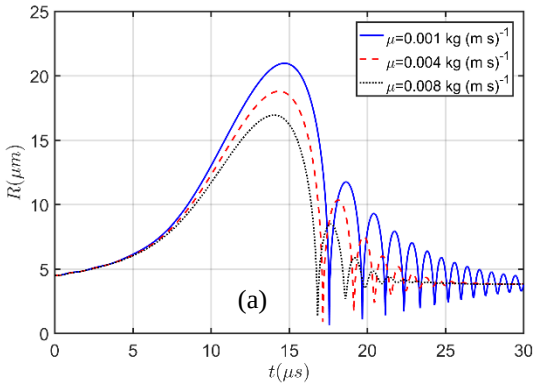

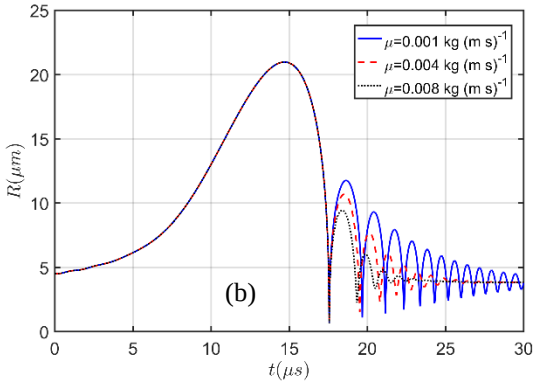

Figure 3: The Bubble radius versus time obtained from numerical solution of KM with speed of sound *C*=1465 (m s)$^{-1}$ the rest of the parameters are the same as in Figure 1. (a) Constant viscosity is μ=0.001, 0.004, 0.008 kg (m s)$^{-1}$. (b) Initial viscosity is μ=0.001 kg (m s)$^{-1}$, at the end of first cycle it changed to 0.004 kg (m s)$^{-1}$ (dashed red line) and 0.008 kg (m s)$^{-1}$ (dotted black line).

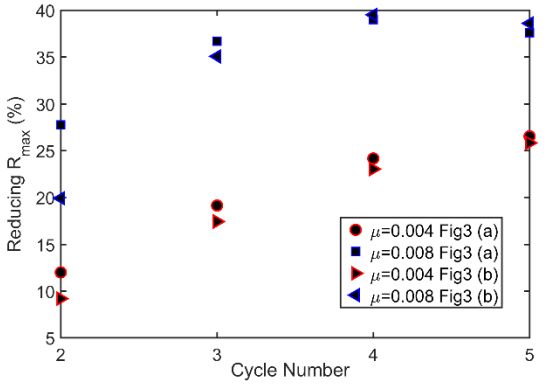

Figure 4: Rate of maximum bubble radius for the cases in Figure 3 versus number of cycles.

Secondly, we use Euler's method to update the density with time as follows:

$$\rho(t+\Delta t)=\rho(t)+\Delta p_L C^2. \qquad (9)$$

Although the liquid (water) is considered as weakly compressible, still small change in the density may has significant effect on the bubble dynamics. Therefore, we used equations (9) and (7) to update the density linearly and nonlinearly respectively at each time steps as can be seen in Figure 5. The compressibility effects more are pronounced when equation (8) is used. The decreasing rate of the maximum bubble radius increase when the equation (8) used instead equation (9).

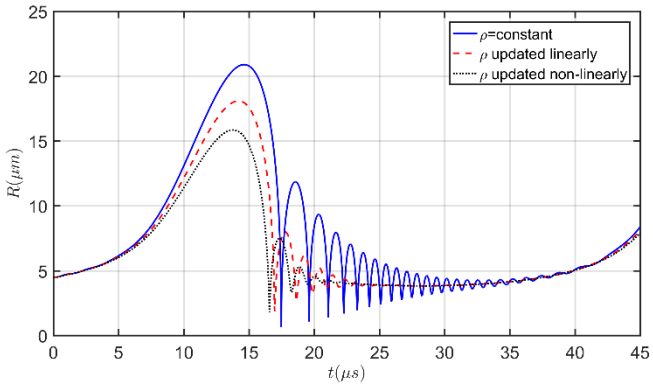

Figure 5: Bubble radius history in compressible liquid by setting ρ=constant=1000 (solid blue line) and using equation (9) (dashed red line) and using equations 7 and 8 (black dotted line).

4. LINEARIZATION OF RPE AND KM

In this section, we assume the oscillation take place around equilibrium radius R_0, so that we can write

$$R(t)=R_0\big(1+x(t)\big), \qquad (10)$$

where $x(t)\ll R_0$. Substituting (10) in (3) and using binomial expansion to give

$$p_b=p_{g0}\left(\frac{1}{1+x(t)}\right)^{3k}$$
$$=p_{g0}\left[1-3kx(t)+\frac{-3k(-3k-1)}{2!}\big(x(t)\big)^2+\cdots\right]. \qquad (11)$$

Equations. (10) and (11) allow us to reformulate RPE in equations (1) for *x* in the form of a linear harmonic-oscillation. Using (10) and (11) in (1) yields,

$$R_0^2[1+x(t)]\,\ddot{x}(t)+\frac{3}{2}R_0^2\dot{x}(t)^2$$
$$=\frac{1}{\rho}\left[\begin{matrix}p_{g0}(1-3kx(t)+\cdots)-p_v-p_\infty-p_\infty\cos(\omega t+\phi)\\ -4\mu(1-x(t)+\cdots)\dot{x}(t)-\frac{2\sigma}{R_0}(1-x(t)+\cdots)\end{matrix}\right] \qquad (12)$$

Neglecting the nonlinear terms in (12) and rearrange it to give harmonic-oscillation equation

$$\ddot{x}+2\beta\dot{x}+\omega_0^2 x=-a\alpha\cos(\omega t+\phi), \qquad (13)$$

where $\alpha=\frac{p_\infty}{\rho R_0^2}$, $\beta=\frac{2\mu}{\rho R_0^2}$ and $\omega_0^2=\frac{1}{\rho R_0^2}\left(3kp_{g0}-\frac{2\sigma}{R_0}\right)$, which can be solved analytically, subject to initial bubble radius and velocity as initial conditions, to allow us to describe the bubble oscillations over

time. The general exact solution of (13) can be expressed as,

$$x(t) = C_1 e^{-t\left(\beta+\sqrt{\beta^2-\omega_0^2}\right)} + C_2 e^{-t\left(\beta-\sqrt{\beta^2-\omega_0^2}\right)} - \frac{a\alpha(\omega_0^2-\omega^2)}{\omega^2-2\omega^2\omega_0^2+4\beta^2\omega^2+\omega_0^4}\cos(\omega t+\phi) - 2\frac{\beta a\alpha\omega}{\omega^2-2\omega^2\omega_0^2+4\beta^2\omega^2+\omega_0^4}\sin(\omega t+\phi). \quad (14)$$

The constants C_1 and C_2 are to be found using the appropriate initial conditions of the bubble. By the same manner with the aid of Maple software (Saeed and Mustafa, 2015), we can simplify the KM equation,

$$\ddot{x} + \beta\dot{x} + \omega_0^2 x = a[\alpha_1 \sin(\omega t+\phi) - \alpha_2\cos(\omega t+\phi)], \quad (15)$$

where

$\alpha_1 = \frac{\omega p_\infty}{\rho R_0 C}, \alpha_2 = \frac{p_\infty}{\rho R_0^2}$,

$\beta = \frac{(CR_0^2 p_{g0}(3k-1)+4C^2R_0\mu+R_0^2p_\infty - aR_0^3 p_\infty \omega \sin\omega t)}{\rho C^2 R_0^3}$ and

$\omega_0^2 = \frac{1}{\rho R_0^2}\left((3kp_{g0}-2\sigma\right)$. Thus the general exact solution can be expressed as,

$$x(t) = C_1 e^{-t\left(\beta+\sqrt{\beta^2-\omega_0^2}\right)} + C_2 e^{-t\left(\beta-\sqrt{\beta^2-\omega_0^2}\right)} - \frac{a(\omega_0^2-\omega^2)[\alpha_2\sin(\omega t+\phi)-\alpha_1\cos(\omega t+\phi)]}{\omega^2-2\omega^2\omega_0^2+4\beta^2\omega^2+\omega_0^4} - 2\frac{\beta a\omega[\alpha_2\sin(\omega t+\phi)+\alpha_1\cos(\omega t+\phi)]}{\omega^2-2\omega^2\omega_0^2+4\beta^2\omega^2+\omega_0^4}.$$

When *C* approach to ∞ Equation (15) reduce to Equation (13).

5. DISCUSSION

The viscosity and compressibility effects are not always negligible in bubble dynamics, particularly at the end of the bubble collapse phases. Both effects lead to bubble radius damping, as we noticed this in all the figures. In the RP and KM, the maximum and minimum bubble radius and cycle period decrease with viscosity and with time, except in the case of μ=0.001 in RP which the minimum bubble radius doesn't change significantly. In the KM when μ=0.001, the maximum bubble radius decreases rapidly, due to considering compressibility effects while in the RP decreases gradually. Furthermore, the exact solutions of the linearization of both models are similar with more terms in the KM due to considering compressibility effects.

6. CONCLUSION

The RP and KM equations describes the spherical bubble motion at infinite fluid for incompressible and compressible liquid, respectively. In this work, we assume that the pressure inside bubble is uniform and it follows adiabatic process. The viscous and compressibility effects in oscillating spherical microbubbles with and without the presence of the acoustic field were investigated for the RP and KM models. Based on the numerical cases, in the RP model, the maximum bubble radius in each cycle reduces linearly with the increasing viscosity, but in KM this was not occurred in all considered cases. Both models are linearized to the harmonic-oscillator equations with the assumptions of small perturbated oscillation and small amplitude of the excited acoustic wave.

References

ABO, A. A., HUSAIN, S. M. & HUSSEIN, S. A. 2018. Effect of Sudden Rise of Water in Stream on Adjacent Land. *ZANCO Journal of Pure and Applied Sciences*, 30**,** 105-112.

BRENNEN, C. E. 2014. *Cavitation and bubble dynamics*, Cambridge University Press.

FRANC, J.-P. & MICHEL, J.-M. 2006. *Fundamentals of cavitation*, Springer science & Business media.

GILMORE, F. R. 1952. The growth or collapse of a spherical bubble in a viscous compressible liquid. *California Institute of Tech Engineering Report*, No. 26-4.

GRIESER, F., CHOI, P.-K., ENOMOTO, N., HARADA, H., OKITSU, K. & YASUI, K. 2015. *Sonochemistry and the acoustic bubble*, Elsevier.

KELLER, J. B. & KOLODNER, I. I. 1956. Damping of underwater explosion bubble oscillations. *Journal of applied physics*, 27**,** 1152-1161.

KELLER, J. B. & MIKSIS, M. 1980. Bubble oscillations of large amplitude. *The Journal of the Acoustical Society of America*, 68**,** 628-633.

KERABCHI, N., MEROUANI, S. & HAMDAOUI, O. 2018. Depth effect on the inertial collapse of cavitation bubble under ultrasound: Special emphasis on the role of the wave attenuation. *Ultrasonics sonochemistry*, 48**,** 136-150.

KOCH, M., LECHNER, C., REUTER, F., KÖHLER, K., METTIN, R. & LAUTERBORN, W. 2016. Numerical modeling of laser generated cavitation bubbles with the finite volume and volume of fluid method, using OpenFOAM. *Computers & Fluids*, 126**,** 71-90.

LAUTERBORN, W. & KURZ, T. 2010. Physics of bubble oscillations. *Reports on progress in physics*, 73**,** 106501.

MANMI, K., WU, W., VYAS, N., SMITH, W., WANG, Q. & WALMSLEY, A. 2020. Numerical investigation of cavitation generated by an ultrasonic dental scaler tip vibrating in a compressible liquid. *Ultrasonics Sonochemistry***,** 104963.

PLESSET, M. S. & PROSPERETTI, A. 1977. Bubble dynamics and cavitation. *Annual review of fluid mechanics,* 9**,** 145-185.

PROSPERETTI, A. & HAO, Y. 1999. Modelling of spherical gas bubble oscillations and sonoluminescence. *Philosophical Transactions of the Royal Society of London. Series A: Mathematical, Physical and Engineering Sciences,* 357**,** 203-223.

SAEED, R. K. & MUSTAFA, A. A. 2015. Homotopy Analysis Method to solve Glycolysis system in one dimension. *ZANCO Journal of Pure and Applied Sciences,* 27**,** 61-70.

SMITH, R., INOMATA, H. & PETERS, C. 2013. *Introduction to supercritical fluids: a spreadsheet-based approach*, Newnes.

VYAS, N., MANMI, K., WANG, Q., JADHAV, A. J., BARIGOU, M., SAMMONS, R. L., KUEHNE, S. A. & WALMSLEY, A. D. 2019. Which parameters affect biofilm removal with acoustic cavitation? A review. *Ultrasound in medicine & biology*.

WANG, Q. 2016. Local energy of a bubble system and its loss due to acoustic radiation. *Journal of Fluid Mechanics,* 797**,** 201-230.

WANG, Q., MANMI, K. & CALVISI, M. L. 2015. Numerical modeling of the 3D dynamics of ultrasound contrast agent microbubbles using the boundary integral method. *Physics of Fluids,* 27**,** 022104.

WANG, Q. X. & MANMI, K. 2014. Three dimensional microbubble dynamics near a wall subject to high intensity ultrasound. *Physics of Fluids*, 26**,** 032104.

YUAN, L., CHENG, H., CHU, M.-C. & LEUNG, P. 1998. Physical parameters affecting sonoluminescence: A self-consistent hydrodynamic study. Physical Review E, 57, 4265.